Desalination and Water Treatment
www.deswater.com
doi: 10.1080/19443994.2014.883332

54 (2015) 316–324
April

Taylor & Francis
Taylor & Francis Group

Effect of NTA and temperature on crystal growth and phase transformations of $CaCO_3$

Shanmukha Prasad Gopi, K. Palanisamy, V.K. Subramanian*

Department of Chemistry, Annamalai University, Annamalainagar, Tamilnadu 608002, India
Tel. +91 94862 82324; email: drvksau@gmail.com

Received 12 August 2013; Accepted 5 January 2014

ABSTRACT

Phase transition from vaterite to calcite is a general behavior of $CaCO_3$ materials. The effect of nitrilotriacetic acid disodium salt (NTA) on the crystallization behavior and polymorphism of $CaCO_3$ was studied at different temperatures between 60 and 230°C. The morphologies and the structure of the precipitates were characterized using scanning electron microscope, field emission scanning electron microscopy, powder X-ray diffraction, Raman spectroscopy, and Fourier transform infrared spectroscopy. It was observed that NTA could change the morphologies and crystal structures of $CaCO_3$ with temperature and stabilize least stable vaterite at high temperature. An anomalous conversion of calcite to vaterite in the presence of NTA was observed. The effect of amount of NTA added on the crystallization behavior at selected temperatures is reported.

Keywords: Crystal growth; Polymorphism; Vaterite; Scale inhibition

1. Introduction

Calcium carbonate ($CaCO_3$) is one of the most abundant mineral in nature. Crystallization of $CaCO_3$ received both scientific and industrial interest and has been widely studied for decades [1,2]. Generally, it exists in six different forms of which three are of anhydrous crystalline forms: calcite, aragonite, and vaterite and three of hydrated forms: amorphous $CaCO_3$ (ACC), calcium carbonate monohydrate ($CaCO_3$ H_2O), and calcium carbonate hexahydrate ($CaCO_3$ $6H_2O$) [3–5]. Among the three crystalline polymorphs, calcite is the thermodynamically most stable followed by metastable aragonite and the least stable vaterite.

The applications of $CaCO_3$ are strictly restricted to its crystalline properties such as chemical purity, specific surface area, particle size, and morphology [1,6–8]. In recent past, synthesis of $CaCO_3$ has been intensively studied with the aim of understanding how crystal polymorph and structural features can be controlled by organic additives [9–11], due to its wide range of applications in paper-making, cosmetics, medicines, detergents, ceramics, rubber, paint, and batch precipitation [12–15].

Despite of its importance, it is also a major constituent in scale found in boilers and heat exchangers [16–18]. Reports suggests that polymorphism plays a vital role in scale formation, i.e. the presence of more calcite in the precipitate can lead to more stable scale and more the vaterite, less stable the scale is [18–21]. Due to this reason, controlling of phase

*Corresponding author.

transformations is very much essential for scale inhibition and as well as for specific polymorph application. The control of polymorphism can be achieved by using certain additives, such as biopolymers, synthetic polymers, fatty acids, and polypeptides containing acidic or basic functional groups [22–24]. In their presence, different crystal forms are kinetically trapped, because of their capability to bind and block out metal ions to control the nucleation, growth, and alignment of materials. Amongst these, nitrilotriacetic acid (NTA) is a synthetic organic metal chelating agent whose metal binding properties are exploited in a broad range of applications i.e. detergent, food, pharmaceutical, cosmetic, metal finishing, photographic, textile, and paper industries and it has found widespread use in conditioning reactor cooling water, as an anticorrosive and scale inhibitor, and in cleanup operations [25,26].

Recently, many studies have reported crystallization of $CaCO_3$ at ambient conditions [16,18,27], but very few details are available at elevated temperatures which simulates conditions inside boilers or other industrial applications. In this paper, we developed a novel approach for the synthesis of $CaCO_3$ using NTA between 60 and 230°C and studied polymorphic transformations at conditions similar to boilers/heat exchangers. The studies displayed an abnormal structure transformation of $CaCO_3$ from bundled needle aragonite to spherical vaterite at low temperatures (>100°C) and triangular pyramidal calcite to spherical vaterite at elevated temperatures i.e. above 200°C. The research offers a novel concept of polymorphic change of aragonite and calcite to spherical vaterite. The findings in this paper could be useful in scale inhibition and de-scaling applications from boilers and heat exchangers.

2. Experimental procedures

2.1. Materials

Analytical grade of $CaCl_2$ and Na_2CO_3 were obtained from Hi-media and NTA from Sigma Aldrich. Double distilled water was used for the preparation of aqueous solutions. The reagents were used as such. Eight samples were prepared in the presence of NTA at different temperatures i.e. 60, 80, 100, 130, 150, 170, 200, and 230°C (S1 to S8).

2.2. Preparation of $CaCO_3$

$CaCO_3$ was crystallized by a modified method from a described one [28]. A typical procedure is as follows: 50 ml 0.1 M $CaCl_2$, 20 ml of 0.1 M NTA, and 60 ml 0.1 N Na_2CO_3 were consecutively added in a Buchner flask, closed tightly with a glass lid to avoid any contamination and kept inside the autoclave. The autoclave was then heated to 60°C for 2 h and the mild precipitate formed was filtered to remove any $CaCO_3$ formed at lower temperatures. The clear solution was kept again in the autoclave and heated to 60°C and kept at the same temperature for 72 h for digestion. Experiments were carried out in the similar way at 80, 100, and 130°C. For synthesis above 130°C, a programmable autoclave manufactured by Thermocon was used and reactions were carried out in Teflon bottles inside the hydrothermal bomb at respective reaction temperature for 72 h. After digestion, autoclave was allowed to cool and the sample was filtered, washed with distilled water, and then dried at 45°C in an oven.

2.3. Characterization

The samples were characterized by Fourier transform infrared spectroscopy (FTIR), Raman, and Powder X-ray diffraction (XRD) techniques to confirm their structure and the morphological studies were done using scanning electron microscope (SEM) and field emission scanning electron microscopy (FESEM). FT–IR spectra were taken in the range of 500–4,000 cm^{-1} using Avatar-330 FTIR and JASCO-5300 FTIR instruments after KBr pelletization. Raman spectra of the samples were obtained with the WI Tec Confocal Raman Microscope alpha 300 R Raman spectrometer, excited by laser line having a wavelength of 633 nm, provided by an argon laser. The XRD patterns were recorded on a Bruker D8 Advanced XRD diffractometer with Cu-Ka radiation at $\lambda = 1.5406$ Å. Microscopic morphological images were taken using Philips XL30-ESEM SEM using a beam voltage of 20 kV and FESEM CARL ZESIS with in-lens detectors. The samples were coated with gold prior to imaging.

3. Results and discussion

3.1. Polymorphic identification and phase confirmation by FTIR spectroscopy and powder diffraction

The crystalline forms of $CaCO_3$ polymorphs were initially identified by FTIR spectroscopy and phase transformations were systematically monitored by powder XRD. It is well known that different crystal forms of $CaCO_3$ show different peaks in FTIR spectrum [29]. The quantification and selection of the appropriate peaks were a difficult task since there is a strong overlapping between these polymorphs. In order to avoid complications arising from

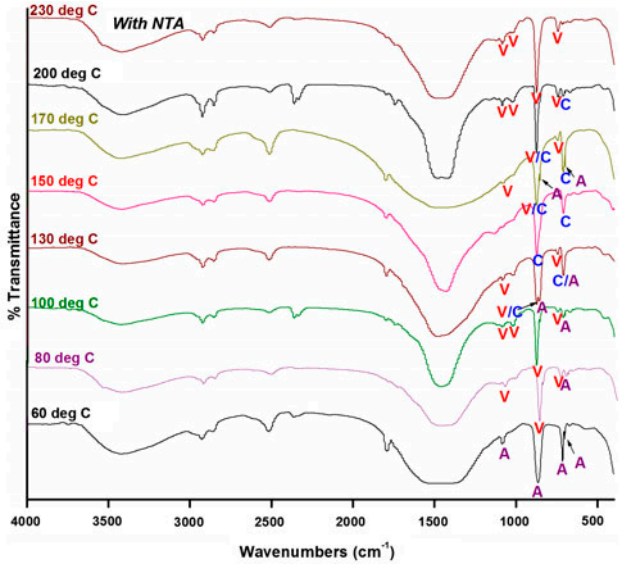

Fig. 1(a). FTIR of $CaCO_3$ synthesized at different temperatures in the presence of NTA.

the overlapping of peaks, FTIR spectra were de-convoluted wherever necessary.

The characteristic carbonate absorption peaks chosen for the different polymorphs in samples are as follows; in-plane bending (ν_4) mode peaks around 700 and 711 cm^{-1} and 745 cm^{-1} for aragonite, calcite and vaterite, respectively; out of plane bending peaks (ν_2 mode) around 856 cm^{-1} for aragonite and at 874 cm^{-1} for both calcite and vaterite; symmetric stretching (ν_1 mode) peaks 1,082 cm^{-1} to aragonite and 1,087 cm^{-1} to vaterite; asymmetric stretching (ν_3 mode) peaks 1,475 and 1,450 cm^{-1} for aragonite and vaterite, respectively [30–32]. In our earlier studies, we have reported that in the absence of any chelating agents, formation of calcite is predominant at higher temperatures above 170°C [28]. FTIR spectra of samples prepared in the presence of NTA are presented in Fig 1(a). Peaks around 700, 856, and 1,082 cm^{-1} confirmed the presence of only aragonite at 60°C. Deconvoluted images are provided in Fig. 1(b) to distinguish aragonite

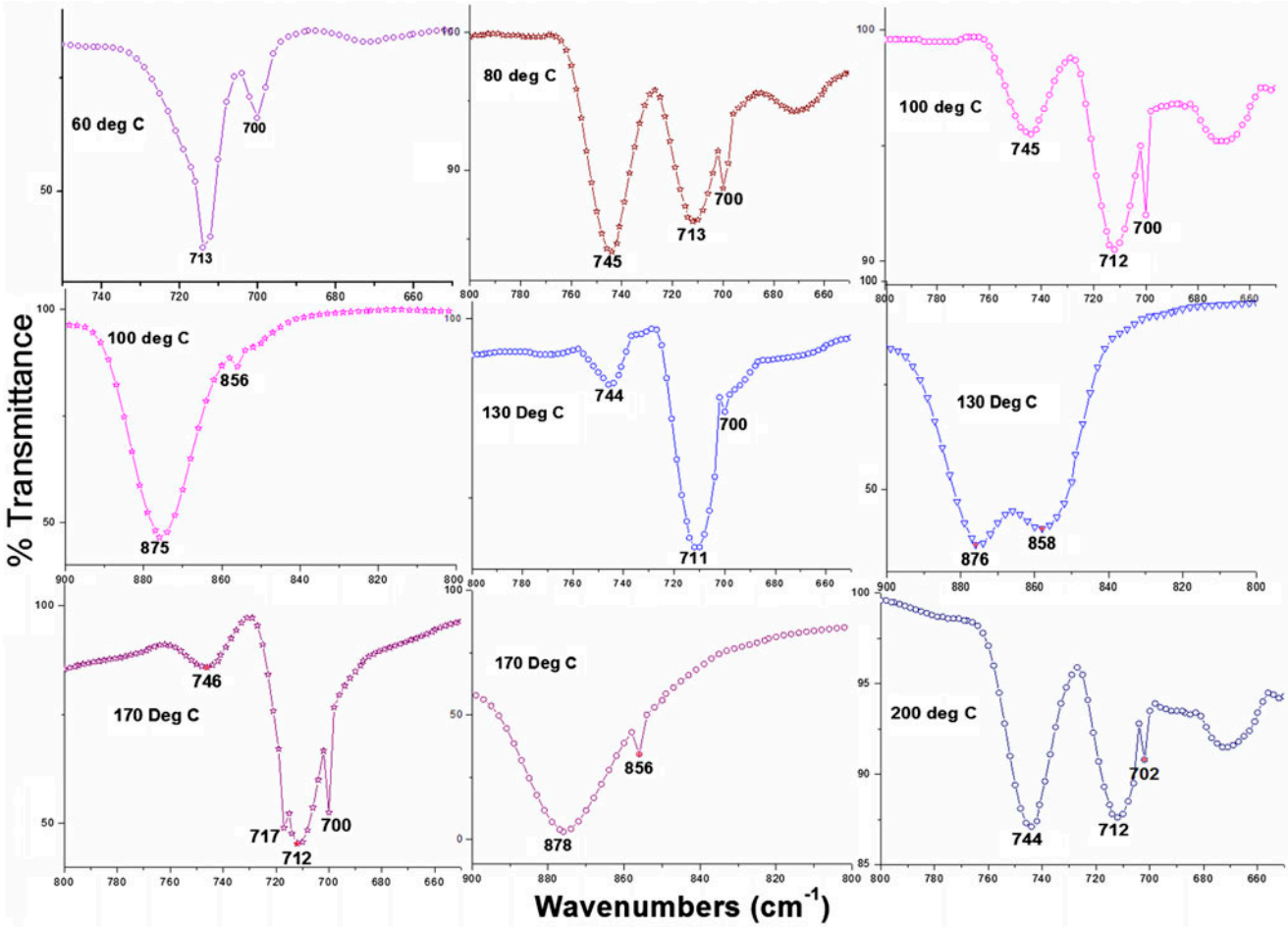

Fig. 1(b). De-convoluted FTIR.

peaks from calcite peaks. With raise in temperature, at 80 and 100 °C, characteristic peak of vaterite at 745 cm^{-1} was observed confirming a binary mixture of aragonite and vaterite in samples S2 and S3. However, at 150 °C, presence of calcite alone was confirmed by presence of its strong peaks at 711 and 876 cm^{-1}. From the above inferences, the development of aragonite leads to calcite with coexistence of vaterite in intermediate samples before the calcite formation at 150 °C. Interesting observations were noticed in phase transformations above 150 °C. Though calcite is of a more stable phase, gradual formation of vaterite was confirmed (peak at 745 cm^{-1}) along with weakening of calcite peak at 711 cm^{-1}, finally resulting pure vaterite above 200 °C.

The quantitative estimation for the transformation of phases was confirmed by using PXRD and the principal peaks corresponding to different phases are highlighted in Fig. 2. The relative amounts of the polymorphic ratio of calcite, aragonite, and vaterite were calculated from the relative areas of the vaterite {110}, calcite {104}, and aragonite {221} by using Kontoyannis equation [33], and are presented in Table 1. It is clear from Table 1 that only aragonite is formed at 60 °C, and at 230 °C mostly vaterite (92%) along with very little aragonite (8%) is formed. Intermediate samples at 80 and 100 °C (S2 and S3) were a binary mixture of vaterite and aragonite. Exceptat 150 °C, where only calcite was present, samples prepared between 130 and 200 °C were composed of a ternary mixture of all the three polymorphs with increasing vaterite with raise in temperature.

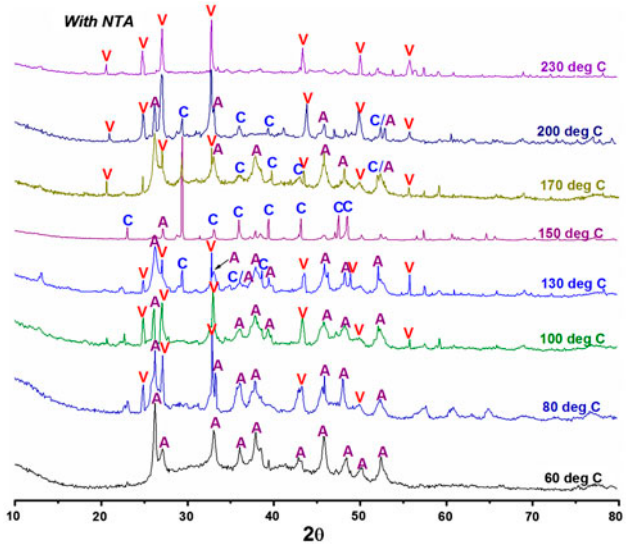

Fig. 2. PXRD pattern of $CaCO_3$ synthesized at different temperatures in the presence of NTA.

Presence of different crystalline polymorphs were confirmed by their characteristic strong diffractions peaks; calcite, aragonite, and vaterite (2θ values) at 29.4° (1 0 4), 26.2° (1 1 1), and 32.7° (0 2 2), (1 1 2), respectively, along with other confirmatory peaks. The XRD patterns are in good agreement with standard JCPDS card numbers 862339, 760606, and 741867 for calcite, aragonite and vaterite, respectively.

It is evident from Fig. 2 that the peaks corresponding to vaterite became stronger with rise in temperature. This shows that the presence of NTA assists the formation of thermodynamically least stable vaterite above 150 °C and this ability increases with temperature. The above inference is further ascertained by Raman and morphological studies.

3.2. Raman spectroscopy

The Raman spectra of the samples are presented in Fig. 3. The Raman bands between 100 and 1,600 cm^{-1} were used to distinguish the polymorphs of $CaCO_3$. The bands observed in the lattice region were assigned as follows: at 217 and 287 cm^{-1} for aragonite, 153 cm^{-1} for calcite and 212 and 302 cm^{-1} to vaterite [34,35]. Further to this, presence of vaterite was confirmed by its most characteristic symmetric stretching (ν_1) band at 1,090 cm^{-1}, and bands at 1,085–1,087 cm^{-1} were assigned for both calcite and aragonite depending upon the presence of other confirmatory bands i.e. in-plane bending, lattice modes, and asymmetric stretching [35]. The differentiations of Raman bands are well noticed in in-plane bending mode and, as well as in asymmetric stretching region above 1,400 cm^{-1}. Band at 702 cm^{-1} (ν_4) and 1,460 (ν_3) were attributed to aragonite, 711 cm^{-1} (ν_4) and 1,434 cm^{-1} (ν_3) to calcite; and 745 cm^{-1} (ν_4), 881 cm^{-1} (ν_2), and 1,441 cm^{-1} (ν_3), to vaterite, respectively. The above vibrational results of $CaCO_3$ polymorphs are well in agreement with FTIR and diffraction studies.

3.3. Morphological studies from SEM

The most common morphologies for different polymorphs of $CaCO_3$ are regular rhomboidal, needle/rod, and spherical for calcite, aragonite, and vaterite, respectively [29,32]. It is already reported that in the absence of any additives, needle/rod/flakes like aragonite with rhomboidal calcite are obtained between 60 and 170 °C and pure rhomboidal calcite above 170 °C [28].

The SEM images of sample prepared at 60 °C are presented in Fig. 4(a) and (b). As could be seen from the magnified image Fig. 4(b), they are agglomerations

Table 1
Molar fraction of $CaCO_3$ polymorphs in presence of NTA and absence of additive at various temperatures (as per Kontoyannis equation)

	Without Additive [29]			With NTA		
Temperature ℃	Calcite	Aragonite	Vaterite	Calcite	Aragonite	Vaterite
60	81	19	00	00	01	50
80	00	00	00	00	33	67
100	12	88	00	00	27	73
130	45	55	00	10	38	52
150	00	00	00	88	12	00
170	00	00	00	10	37	53
200	95	05	00	08	21	71
230	97	03	00	00	08	92

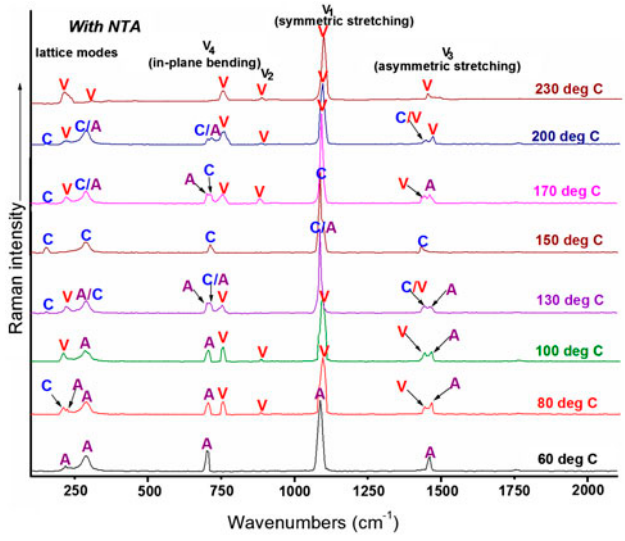

Fig. 3. Raman spectra of $CaCO_3$ synthesized at different temperatures in the presence of NTA.

of fine micro needle-like structures. From XRD, FTIR, and Raman studies it could be deduced that these are aragonite. The SEM images of samples at 80 and 100℃ are shown in Fig. 4(c) and (d), respectively. It was observed that the morphology changed more to spherical with temperature, confirming tendency for conversion into vaterite. This trend is observed in XRD, FTIR, and Raman studies also. A major change in the morphology was observed at 130℃ (Fig. 4(e)). A combination of three different morphologies, trigonal pyramidal, spherical, and needle-like spheres are present in the image. XRD, FTIR, and Raman studies revealed presence of all the three polymorphs in this sample. The FESEM of sample at 150℃ is presented in Fig. 4(f). The sample contained only calcite and the FESEM also showed single morphology of trigonal pyramidal structures having size ranging from 100 to about 800 nm. From this it could be inferred that the trigonal pyramidal morphology in Fig. 4(e) also belongs to calcite. SEM image of the sample at 170℃ showed deformation of trigonal pyramidal calcite structure and appearance of spherical vaterite particles (Fig. 4(g)). Further increase in temperature (200℃) resulted again in three different morphologies (Fig. 4 (h)). These data are in good agreement with XRD, Raman, and FTIR results. Appearance of exclusive spherical structures (Fig. 4(i)) confirmed presence of vaterite alone in the sample at 230℃.

3.4. Mechanism

From the above, it is now clear that NTA significantly influences the crystallization process of $CaCO_3$ and is influenced by temperature. Though nothing can be said at this stage on the possible mechanism of inter-conversion of different polymorphs of $CaCO_3$, it is obvious that the process undergoes stages which violate the Ostwald's rule of stages. Our earlier studies have also demonstrated that $CaCO_3$ does not follow the Ostwald's rule of stages at elevated temperatures in the presence of chelating agents. Generally, temperature influences the interaction between additive and calcium ions and plays a vital role in stabilizing different polymorphs (by affecting nucleation, crystal growth etc.) and thereby the morphology of $CaCO_3$. In most of the cases additives may favor phase transformations towards metastable forms in normal conditions i.e. low temperatures, but very few and effective additives can control the regular growth and favor the least stable phase at elevated temperatures [36–38]. In the presence of NTA, the crystal growth initially stabilizes aragonite, and with the increase of temperature at 100℃ vaterite is stabilized and between 130 and 200℃ growth of calcite is favored, above which vaterite alone is crystallized.

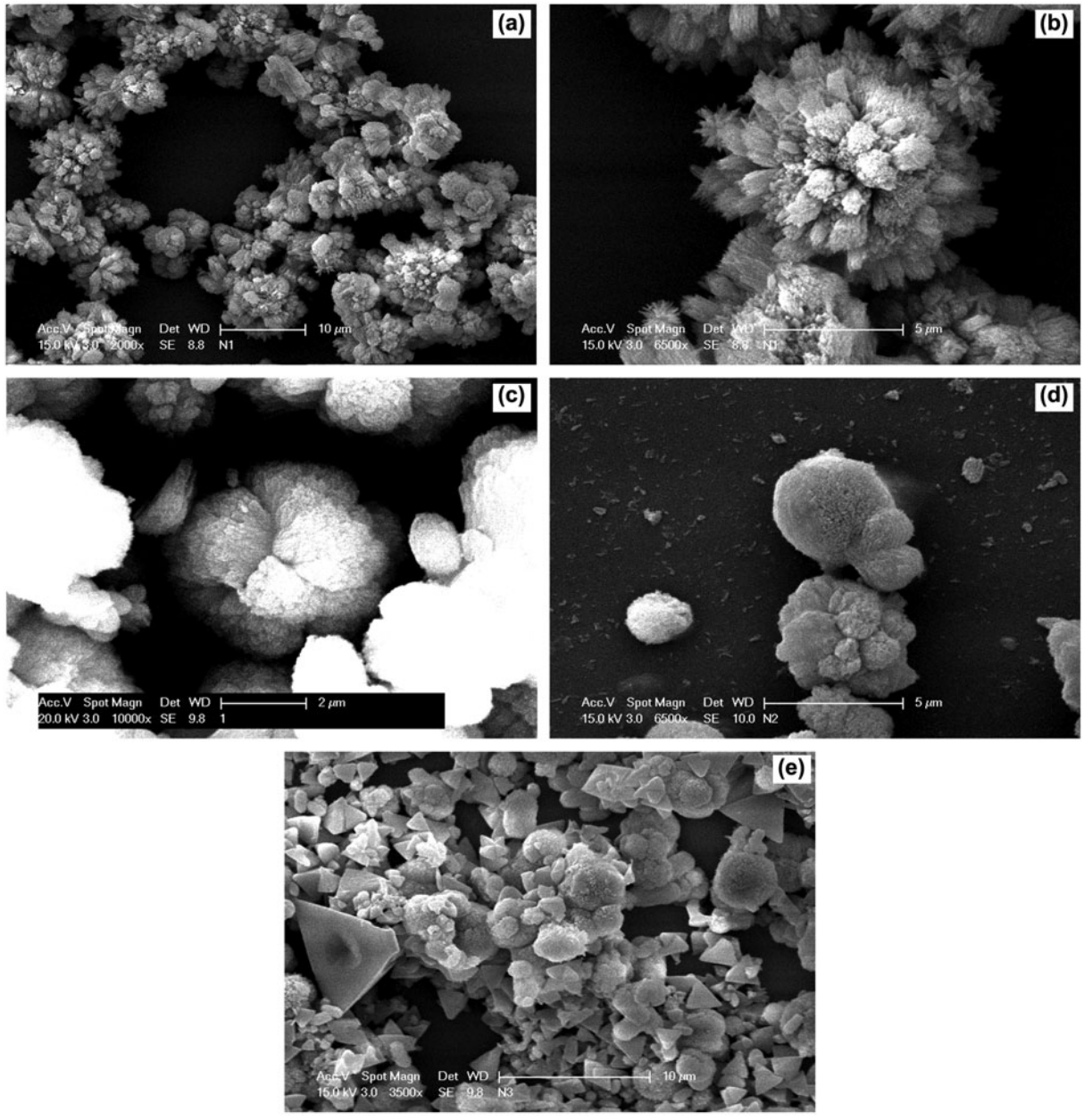

Fig. 4. SEM images of $CaCO_3$ synthesized at different temperatures in the presence of NTA.

Usually the crystallization of $CaCO_3$ will start instantaneously after the addition of calcium chloride to sodium carbonate because of the fast reaction of crystallization, but addition of NTA results into the formation of complex, thereby necessitating a high supersaturation level than normal to form precipitate. As a result, ACC which was first generated through the initial crystallization took a different course during the nucleation process through the dissolution mechanism. The general mechanism suggested for stabilizing the metastable forms (for scale inhibition) is that, the inhibitor functional groups exhibit a significant impact on the inhibitory power in terms of controlling the scale precipitation, i.e. adsorption calcium to NTA on the crystal surface, which blocks the active crystal growth sites. After the adsorption phase, several modes of actions are considered: delaying germination, slow-down crystal growth rate, giving them a friable structure that weakens its adherence to a flow surface etc [18]. Probably here, the interaction

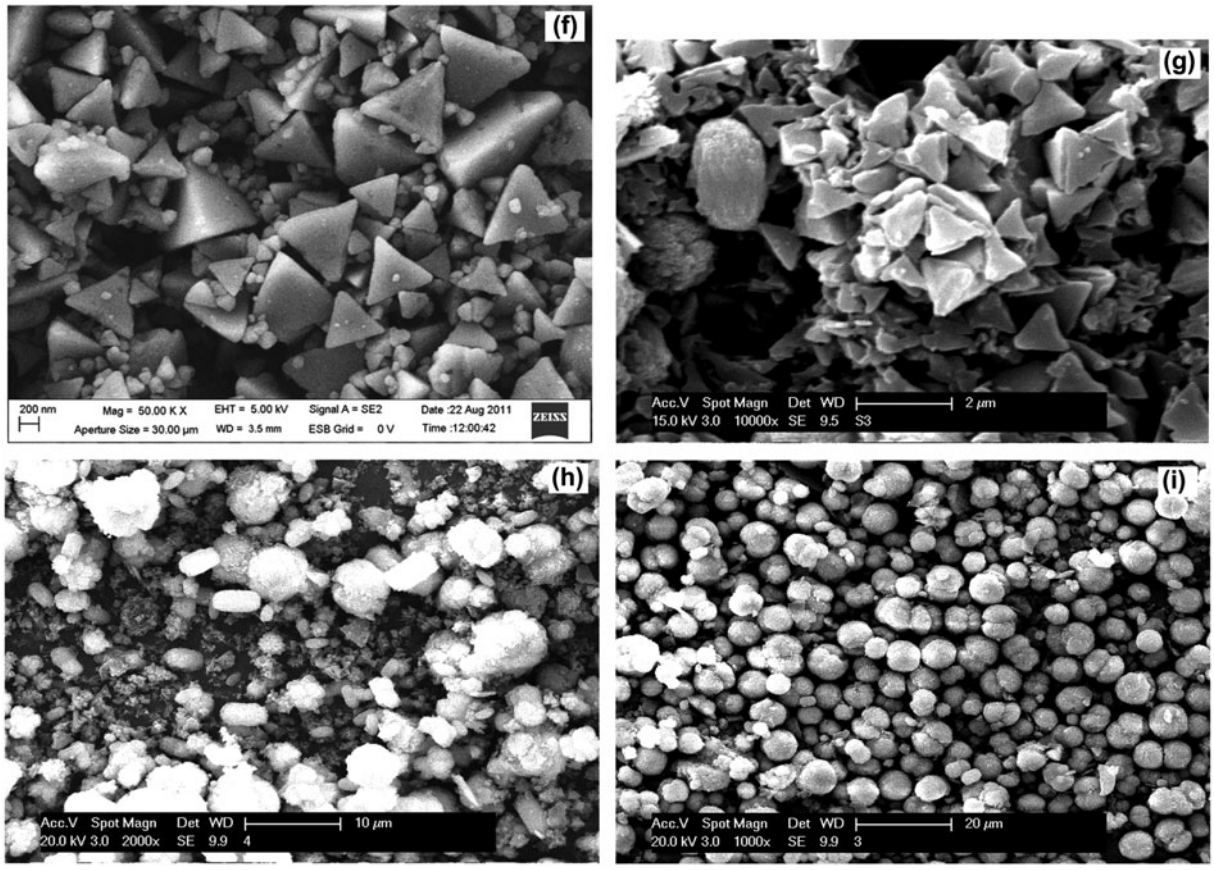

Fig. 4. (*Continued*).

between Ca^{2+} ions with NTA could have lowered the interface energy and caused the conditions to be kinetically controlled, leading to preferred nucleation of metastable polymorphs or least stable polymorph. As per the Ostwald rule in crystallization, less stable crystalline forms may nucleate than thermodynamically stable forms since kinetics are often more important than thermodynamics in non-equilibrium precipitating systems [9]. So, during $CaCO_3$ crystal growth, the inhibitor molecules disturb the regular outgrowth of $CaCO_3$ crystals. This can satisfactorily explain the formation of a binary mixture of calcite and aragonite (below 200˚C) and only calcite (at 200 and 230˚C) in the absence any additives and NTA's influence on controlling the nucleation growth and thereby, facilitating the formation of metastable phases at different temperatures.

4. Conclusion

The influence of NTA and temperature on the nature of the polymorph that precipitates during crystallization of $CaCO_3$ from $CaCl_2$ using Na_2CO_3 has been investigated extensively. The results presented here demonstrate the formation of pure aragonite and vaterite at 60 and 230˚C, respectively, thus revealing new and simple route to synthesize them. It is also noticed that NTA has better control over the phase transformations at elevated temperatures which increases its chelating ability and make it suitable for practical applications such as boiler scale control/sludge removal in industries.

Acknowledgment

We express our sincere thanks to the University Grants Commission (UGC), New Delhi, India, for financial support through Major Research Project (37-40/2009 (SR) dated 12.01.2010). We are also grateful to UGC Networking Resource Centre, University of Hyderabad, Hyderabad, India for providing facilities for carrying out the instrumental analysis.

References

[1] X. Yang, G. Xu, The influence of xanthan on the crystallization of calcium carbonate, J. Cryst. Growth 314 (2011) 231–238.

[2] H. Tang, J. Yu, X. Zhao, Controlled synthesis of crystalline calcium carbonate aggregates with unusual morphologies involving the phase transformation from amorphous calcium carbonate, Mater. Res. Bull. 44 (2009) 831–835.

[3] H. Cölfen, Precipitation of carbonates: Recent progress in controlled production of complex shapes, Curr. Opin. Colloid Interface Sci. 8 (2003) 23–31.

[4] S. Arpita, S. Mahapatra, Synthesis of all crystalline phases of anhydrous calcium carbonate, Cryst. Growth Des. 5 (2010) 2129–2135.

[5] A. Antony, J.H. Low, S. Gray, A.E. Childress, P. Le-Clech, G. Leslie, Scale formation and control in high pressure membrane water treatment systems: A review, J. Membr. Sci. 383 (2011) 1–16.

[6] M. Vučak, M.N. Pons, J. Perić, H. Vivier, Effect of precipitation conditions on the morphology of calcium carbonate: Quantification of crystal shapes using image analysis, Powder Technol. 97 (1998) 1–5.

[7] S.R. Dickinson, G.E. Henderson, K.M. McGrath, Controlling the kinetic versus thermodynamic crystallisation of calcium carbonate, J. Cryst. Growth 244 (2002) 369–378.

[8] M. Mihai, M.D. Damaceanu, M. Aflori, S. Schwarz, Calcium carbonate microparticles growth templated by an oxadiazole-functionalized maleic anhydride-co-n-vinyl-pyrrolidone copolymer, with enhanced ph stability and variable loading capabilities, Cryst. Growth Des. 12 (2012) 4479–4486.

[9] S.R. Payne, M.H. Butler, M.F. Butler, Formation of thin calcium carbonate films on chitosan biopolymer substrates, Cryst. Growth Des. 7 (2007) 1262–1276.

[10] X. Yang, G. Xu, $CaCO_3$ crystallization controlled by (2-hydroxypropyl-3-butoxy) propylsuccinyl chitosan, Powder Technol. 215–216 (2012) 185–194.

[11] M. Cusack, A. Freer, Biomineralization: Elemental and organic influence in carbonate systems, Chem. Rev. 108 (2008) 4433–4454.

[12] Z. Nan, B. Yan, X. Wang, R. Guo, W. Hou, Fabrication of calcite aggregates and aragonite rods in a water/pyridine solution, Cryst. Growth Des. 8 (2008) 4026–4030.

[13] L. Xiang, Y. Xiang, Y. Wen, F. Wei, Formation of $CaCO_3$ nanoparticles in the presence of terpineol, Mater. Lett. 58 (2004) 959–965.

[14] D. Walsh, S. Mann, Fabrication of hollow porous shells of calcium carbonate from self-organizing media, Nature 377 (1995) 320–323.

[15] S.F. Chen, S.H. Yu, T.X. Wang, J. Jiang, H. Cölfen, B. Hu, B. Yu, Polymer-directed formation of unusual $CaCO_3$ pancakes with controlled surface structures, Adv. Mater. 17 (2005) 1461–1465.

[16] Z. Wu, J.H. Davidson, L.F. Francis, Effect of water chemistry on calcium carbonate deposition on metal and polymer surfaces, J. Colloid Interface Sci. 343 (2010) 176–187.

[17] J.H. Low, S. Gray, A.E. Childressc, P.L. Clech, G. Leslie, Scale formation and control in high pressure membrane water treatment systems: A review, J. Membr. Sci. 383 (2011) 1–16.

[18] R. Ketrane, B. Saidani, O. Gil, L. Leleyter, F. Baraud, Efficiency of five scale inhibitors on calcium carbonate precipitation from hard water: Effect of temperature and concentration, Desalination 249 (2009) 1397–1404.

[19] Z.G. Cai, J. Ge, M.Q. Sun, B.L. Pan, T. Mao, Z.Z. Song, Investigation of scale inhibition mechanisms based on the effect of scale inhibitor on calcium carbonate crystal forms, Sci. China B Chem. 50 (2007) 114–120.

[20] K.J. Westin, H.C. Rasmuson, Precipitation of calcium carbonate in the presence of citrate and EDTA, Desalination 159 (2003) 107–118.

[21] Y.P. Lin, P.C. Singer, Inhibition of calcite crystal growth by polyphosphates, Water Res. 39 (2005) 4835–4843.

[22] F.C. Meldrum, S.T. Hyde, Morphological influence of magnesium and organic additives on thepre cipitation of calcite, J. Cryst. Growth 231 (2001) 544–558.

[23] X. Liu, L. Zhang, Y. Wang, C. Guo, E. Wang, Biomimetic crystallization of unusual macroporous calcium carbonate spherules in the presence of phosphatidylglycerol vesicles, Cryst. Growth Des. 8 (2008) 759–762.

[24] S.E. Wolf, J. Leiterer, M. Kappl, F. Emmerling, W. Tremel, Carbonate-coordinated metal complexes precede the formation of liquid amorphous mineral emulsions of divalent metal carbonates, J. Am. Chem. Soc. 130 (2008) 12342–12347.

[25] Y.V. Nancharaiah, N. Schwarzenbeck, T.V.K. Mohan, S.V. Narasimhan, P.A. Wilderer, V.P. Venugopalan, Biodegradation of nitrilotriacetic acid (NTA) and ferric–NTA complex by aerobic microbial granules, Water Res. 40 (2006) 1539–1546.

[26] V.E. White, C.J. Knowles, Degradation of copper-NTA by Mesorhizobium sp. NCIMB 13524, Int. Biodeterior. Biodegrad. 52 (2003) 143–150.

[27] J.H. Guo, S.J. Severtson, Application of classical nucleation theory to characterize the influence of carboxylate-containing additives on $CaCO_3$ nucleation at high temperature, pH, and ionic strength, Ind. Eng. Chem. Res. 42 (2003) 3480–3486.

[28] S.P. Gopi, V.K. Subramanian, Polymorphism in $CaCO_3$—Effect of temperature under the influence of EDTA (di sodium salt), Desalination 297 (2012) 38–47.

[29] L.M. Qi, J. Li, J. Ma, Biomimetic morphogenesis of calcium carbonate in mixed solutions of surfactants and double-hydrophilic block copolymers, Adv. Mater. 14 (2002) 300–303.

[30] F.A. Andersen, L. Brečević, Infrared spectra of amorphous and crystalline calcium carbonate, Acta Chem. Scand. 45 (1991) 1018–1024.

[31] N.V. Vagenas, A. Gatsouli, C.G. Kontoyannis, Quantitative analysis of synthetic calcium carbonate polymorphs using FT-IR spectroscopy, Talanta 59 (2003) 831–836.

[32] S.F. Chen, S.-H. Yu, J. Jiang, F. Li, Y.K. Liu, Polymorph discrimination of $CaCO_3$ mineral in an ethanol/water solution: Formation of complex vaterite superstructures and aragonite rods, Chem. Mater. 18 (2006) 115–122.

[33] C.G. Kontoyannis, N.V. Vagenas, Calcium carbonate phase analysis using XRD and FT-Raman spectroscopy, Analyst 125 (2000) 251–255.

[34] M.M. Tlili, M.B. Amor, C. Gabrielli, S. Joiret, G. Maurin, P. Rousseau, Characterization of $CaCO_3$ hydrates by micro-Raman spectroscopy, J. Raman Spectrosc. 33 (2001) 10–16.

[35] U. Wehrmeister, A.L. Soldati, D.E. Jacob, Raman spectroscopy of synthetic, geological and biological vaterite: A Raman spectroscopic study, J. Raman Spectrosc. 41 (2010) 193–201.
[36] Z. Chen, Z. Nan, Controlling the polymorph and morphology of $CaCO_3$ crystals using surfactant mixtures, J. Colloid Interface Sci. 358 (2011) 416–422.
[37] J. Yu, M. Lei, B. Cheng, X. Zhao, Facile preparation of calcium carbonate particles with unusual morphologies by precipitation reaction, J. Cryst. Growth 261 (2004) 566–570.
[38] J. Chen, L. Xiang, Controllable synthesis of calcium carbonate polymorphs at different temperatures, Powder Technol. 189 (2009) 64–69.